High power (>1 W) room-temperature (300 K) 980 nm continuous-wave AlGaAs/InGaAs/GaAs semiconductor lasers

Kamil KOSIEL*, Jan MUSZALSKI, Anna SZERLING, Maciej BUGAJSKI

Institute of Electron Technology, al. Lotników 32/46, 02-668 Warsaw, Poland

*Corresponding author: kosiel@ite.waw.pl

A technology of high power, continuous-wave (CW) semiconductor lasers has been elaborated. AlGaAs/InGaAs/GaAs heterostructures, grown by molecular beam epitaxy (MBE), were used to fabricate laser diodes. The active region of laser diode was formed as strained, 8 nm thick, quantum well (QW) InGaAs layer. The AlGaAs layers of graded composition and graded refractive index (GRIN) formed the waveguide. Lasers were processed into wide stripe ($W = 100$ μm) mesas and were mounted on copper submounts and Peltier thermoelements in the standard TO-3 transistor housing. For stabilization of laser output, a silicon photodiode was placed next to a laser chip in the same case. Typical threshold current densities were 150 A/cm^2, and the quantum efficiencies were of the order of 0.8 W/A. Lasers may work in pulsed regime as well as in CW regime with guaranteed optical power of 1 W at 300 K. The record threshold current densities achieved for 700 μm cavity were as low as 130 A/cm^2 and the characteristic temperature was $T_0 = 200$ K.

Keywords: high power semiconductor laser, graded refractive index separate confinement heterostructure (GRINSCH), threshold current, external efficiency, parameter T_0, Auger recombination, spontaneous radiative recombination, nonradiative recombination.

1. Introduction

The graded refractive index separate confinement heterostructure (GRINSCH) laser is probably the best construction type for an edge emitter. It shows superior basic parameters, particularly important in case of high power laser diodes, *i.e.*, threshold current I_{th}, external differential efficiency η_{ext}, and parameter T_0. The characteristic temperature T_0 describes the dependence of laser threshold current on temperature:

$$I_{th}(T + \Delta T) = I_{th}(T) \exp(\Delta T/T_0) \qquad (1)$$

GRINSCH structure is better, in particular, than the "classical" separate confinement heterostructure (SCH) with the rectangular shape of a bandgap profile. The GRINSCH construction advantages are mainly the result of suppressing the carrier

losses by the internal electric field, built in the heterostructure. The field is related to the graded composition (GRIN – graded index) waveguide region.

Firstly, the losses mentioned above result from the leakage of carriers "through" the states of higher energy, which form continuum of states. This leaking of a portion of carriers, injected in the p-i-n structure to the other than QW regions, makes them lost because of the simple spatial separation from the active region. This is followed, however, by some other phenomena which have recombinational nature and are detrimental from our point of view as they result in further carrier losses [1, 2]. They are: Auger recombination [3–5], spontaneous radiative recombination, and nonradiative recombination. The last one is described by a Shockley–Read–Hall (SRH) model. The contributions to the carrier losses are found in an expression for the threshold current density:

$$j_{th} = ed\left(An_{th} + Bn_{th}^2 + Cn_{th}^3\right) + j_{leak} \tag{2}$$

where e is the elemental charge, d is the thickness of the pumped region, n_{th} is minority carriers density, j_{leak} is the density of leakage current, A may be interpreted as nonradiative recombination coefficient and B, C are, respectively, radiative spontaneous and Auger recombination coefficients. According to the accepted nature of A, we may understand it as:

$$A = \tau^{-1} = N\sigma v \tag{3}$$

where τ means carrier lifetime, N is the density of the centres of nonradiative recombination (deep traps), σ is the cross-section for electron capture by traps, and v is the carrier velocity.

The rates of recombination processes depend on the concentration of minority carriers, so in a QW it is a few orders of magnitude higher than in any other region of the laser structure. This simply results from the formation of potential minimum in the QW and consequently from the highest value of carrier concentration in it. However, because a waveguide region is usually about two orders of magnitude thicker than a QW, the intensity of recombination in a waveguide may significantly contribute to the global process. This is particularly important in the case of a relatively low QW barrier, when in the condition of high injection level, which is necessary for laser action, also the waveguide is filled to appreciable concentration with electrons and holes. The example is the AlGaAs/InGaAs/GaAs 980-nm laser heterostructure presented in this paper, with InGaAs/GaAs barrier of about 0.120 eV in the conduction band.

The smallest intensity of recombination processes is observed in doped regions, like laser claddings, because of very low concentration of minority carriers [6].

The same reasons which lead to the decrease in the I_{th} cause also fast increase in internal efficiency η_i above the threshold, which manifests itself in a steep $P(I)$, characteristic above threshold.

The higher is the electric field built into the heterostructure, the smaller amount of carriers in a pumped region is necessary for fulfilling the lasing condition. Therefore the field is also a factor which improves external efficiency η_{ext} of the laser by reduction of free carrier absorption.

The increase in carrier leakage and recombination processes accompanying the leakage, with temperature, are the reasons of decreasing parameter T_0. The GRINSCH structure allows to obtain higher T_0.

All the benefits of applying the GRINSCH structure, however, may be reduced or even lost in case of poor epitaxial material quality, for example, high concentration of nonradiative recombination centres. This fact shows how important is the appropriate technology of epitaxy. What is more, there is a close linkage between the used construction and technology. The two aspects must be considered together, and in the optimization process, local and technological circumstances have to be taken into account.

In the case of III–V materials, the oxygen is known to be an important nonradiative recombination center [7]. This effect is particularly strong in layers containing Al, because of great chemical affinity of these elements. The problem is growing in importance with the rise in minority carrier concentration which is present in so contaminated layer during lasing. A discussion about constructional and technological aspects of laser structures, concerning mainly the waveguide regions and the presence of oxygen was published in [6]. In this paper we consider the structures grown in conditions that minimize oxygen content and concentrate on the role of exact GRIN profile in high power, CW lasers. Two AlGaAs/InGaAs/GaAs GRINSCH constructions, which vary in the GRIN profile, are discussed.

2. Experimental

In two tested GRINSCH constructions (Fig. 1), the QW undoped active region consisted of the 8 nm thick $In_{0.20}Ga_{0.80}As$ layer embedded in the middle of 10 nm GaAs and subsequently placed in the centre of 900 nm thick graded composition (graded index – GRIN) waveguide layers, surrounded by doped (n-type and p-type), 1.2 µm thick $Al_{0.28}Ga_{0.72}As$ layers. In the GRIN layers, the aluminium content varied in the range of 0–28%, however they differed in shape. The construction A had U-shaped composition profile, while in the structure B the composition profile was linear.

Si and Be were used for n- and p-type doping, respectively. The n- and p-type doping levels were the same for both investigated structures. The free electron concentration was 5×10^{17} cm^{-3} in n-type $Al_{0.28}Ga_{0.72}As$, while the hole concentration in p-type $Al_{0.28}Ga_{0.72}As$ layers was close to 1×10^{18} cm^{-3}.

The laser heterostructures were grown by solid source molecular beam epitaxy (SS MBE) technique in Riber Compact 21T reactor. Nominally (100) oriented GaAs n$^+$ substrates supplied by AXT were used. The valved-cracker As effusion cell producing As$_2$ molecules was used. For the third group elements, the ABN 80 DF
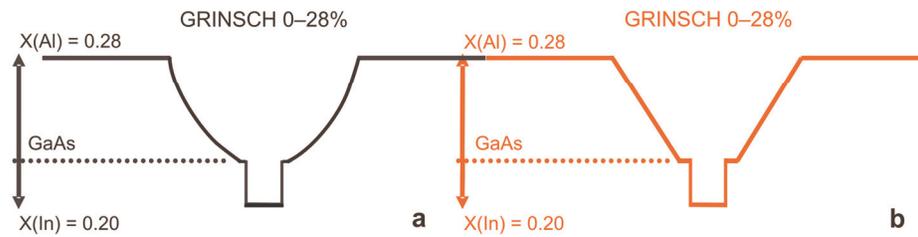
Fig. 1. Composition profiles of $Al_xGa_{1-x}As$ (over the GaAs level) and $In_xGa_{1-x}As$ (under the GaAs level) for heterostructures A (**a**) and B (**b**). Cladding regions are characterized by constant composition of AlGaAs.

effusion cells were used. Growth rate of GaAs was 1 μm/h. The substrate temperature T_s, controlled on the surface of a growing crystal by a pyrometer, was kept at 550 °C, 580 °C and 690 °C during epitaxy of InGaAs, GaAs and AlGaAs layers, respectively. The construction B was realized once, while the construction A was implemented in three epitaxial structures grown in nominally the same technological conditions. The exact T_s profiles, used during epitaxy of heterostructures, are shown together with appropriate composition profiles in Fig. 1. Before and after InGaAs QW layer deposition, the crystal growth was interrupted in all cases and the T_s value was changed gradually between neighbouring layers. Such rather high T_s, used for deposition of all layers which contain Al, was found necessary to avoid considerable oxygen contamination [6].

The epi-wafers were processed into oxide isolated, ridge waveguide, wide stripe lasers with stripe width of 100 μm. The laser diodes, processed with mesas formed by wet etching, had the resonator length of 700 μm, p-type (Pt/Ti/Pt/Au) and n-type (AuGe/Ni/Au) metallic contacts. The lasers with uncoated mirrors were fabricated. The last fact means that one has to keep in mind that all measured quantities refer to the single mirror output and the total generated optical power and quantum efficiency are roughly doubled with appropriate antireflective and high reflective coatings. Light-current characteristics (P-I) and current-voltage characteristics (I-V) were measured in CW conditions as well as pulse supply conditions, with following parameters of supply: maximum current amplitude $I_{ps} = 2$ A, pulse filling factor ff $= 0.1\%$, pulse duration $\tau = 500$ ns, pulse frequency $\nu = 2$ kHz.

Oxygen concentration profiles in the epitaxial structures were investigated by secondary ion mass spectrometry (SIMS) technique, etching the samples with Cs^+ beam and with energy of 14.5 keV. The oxygen concentration calibration was obtained by measurements of $^{16}O^-$ isotope signal and $^{75}As^-$ signal as a reference. Relative sensitivity factor (RSF) used to determine the concentration was identified on the basis of suitable standards, *i.e.*, AlGaAs and GaAs layers implanted with oxygen.

The experimental results were interpreted on the basis of device simulations made with PICS3D software [8]. The calculations were based on drift-diffusion model including quantum mechanical treatment of QW active region. An assumption of the same lifetime of electron-hole pairs in all regions of all analysed constructions

have been made. In the case of nonradiative recombination, according to the accepted SRH model, this corresponds to the assumption of the same nature of deep traps in all regions, *i.e.*, the same cross-section for the nonradiative process and the same concentration of the trap states. The computational model neglects heating effects, *i.e.*, calculations are isothermal. Bimolecular recombination (B) and Auger (C) coefficients, present in the expression for the threshold current, were selected on the basis of extensive literature search. Their values were confronted with those given in the manual for the PICS3D software for (In)GaAs material.

3. Results and discussion

All investigated structures lased in pulse (Fig. 2) as well as in CW mode (Fig. 3) at room-temperature (300 K). Structures with linear GRIN profile exhibited lower

Fig. 2. Optical power-current, pulse, room-temperature (300 K) characteristics, for two sets of structures presented in the paper. Total power, *i.e.*, from the two mirrors, is presented.
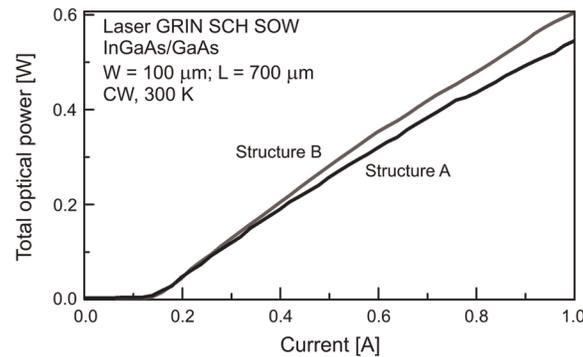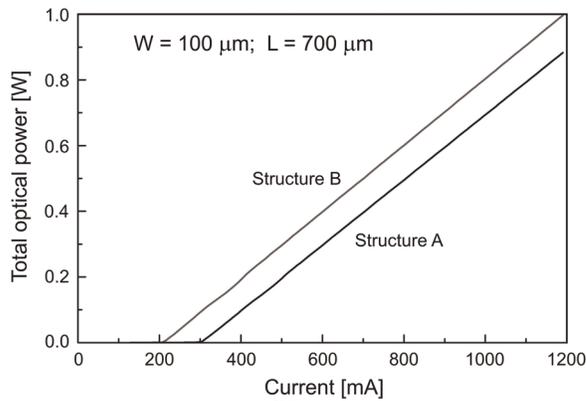

Fig. 3. Optical power-current, CW, room-temperature (300 K) characteristics, for two selected structures presented in the paper. Total power, *i.e.*, from the two mirrors, is presented.

average threshold I_{th} and generally higher external differential efficiency η_{ext} and characteristic temperature T_0 than the structure with U-shaped waveguide. This is clearly seen when one compares the best, selected laser chips, as well as average values of given parameters (*cf.*, Figure 2 and the Table). This effect is consistent

T a b l e. Record and average values of threshold current, external diferential efficiency and T_0 for the heterostructures of interest.

Structure	I_{th} [mA]	$I_{th,av}$ [mA]	η_{ext} [W/A]	$\eta_{ext,av}$ [W/A]	T_0 [°C]	$T_{0,av}$ [°C]
A	120	140	1.20	0.96	160	130
B	100	120	1.40	1.10	200	160

Fig. 4. Simulated optical power-current, isothermal room-temperature (300 K) characteristics, for two constructions presented in the paper. Total power, *i.e.*, from the two mirrors, is presented.
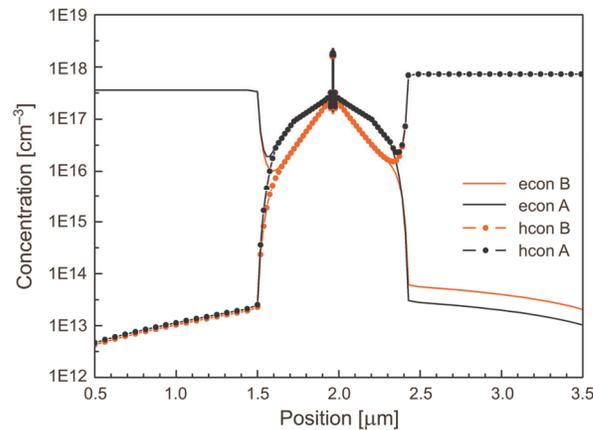

Fig. 5. Calculated carrier concentration in the laser's active region. For simulation details see the legend in the inset – econ and hcon concern, respectively, electron and hole concentration; letters A or B relate to the given structure.

with the theoretical predictions of lower I_{th} value for structure B (Fig. 4). Qualitatively modeled decrease in I_{th} for this laser construction is explained as being the result of lower n- and p-type carrier concentration in the waveguide region (Fig. 5). This is the reason of lower recombination rates of detrimental recombination processes (Fig. 6).

Oxygen concentration in the heterostructure does not exceed 10^{17} cm^{-3}, however in cladding AlGaAs layers it is a few times higher than in GaAs. In a waveguide, *i.e.*, graded composition AlGaAs, oxygen concentration goes through the range of middle values (Fig. 7). They were on average slightly higher for the structure B in a waveguide,
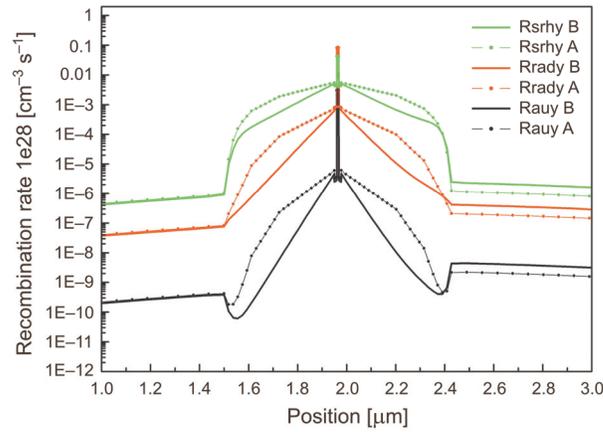

Fig. 6. Calculated recombination rates: nonradiative SRH, Auger and spontaneous radiative. For simulation details see the legend in the inset – Rsrhy, Rrady and Rauy concern, respectively, nonradiative, spontaneous and Auger recombination; letters A or B relate to the given structure.
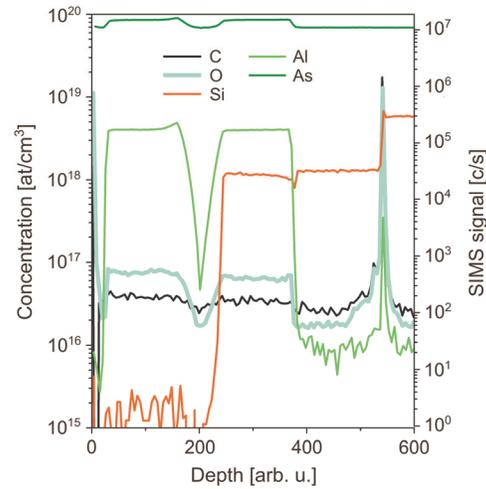

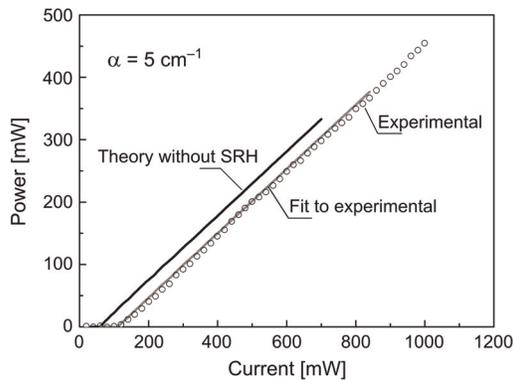Fig. 7. Elemental concentration profiles measured by SIMS for structure A.

Fig. 8. Experimental and simulated optical power-current, isothermal room-temperature (300 K) characteristics. Total power, *i.e.*, from the two mirrors, is presented.

so one may find it to be a contribution to the degradation of laser properties. It is clear, however, that it is not a predominant effect.

For a quantitative evaluation of the laser heterostructure parameters, the experimental P-I characteristics were fitted with theory. The extracted value of internal losses α_i, which influence the slope of the characteristic, is 6 cm^{-1} (5 cm^{-1} related to free carrier absorption and 1 cm^{-1} connected with scattering on defects), whereas that of the carrier lifetime τ equals 5 ns (Fig. 8).

To quantify the probable effect of nonradiative recombination on the optical power, the typical experimental $P(I)$ characteristic was compared to the theoretical one, calculated with the assumption of a lack of SRH recombination (Fig. 8). Such predicted threshold current which is about 1.8 times lower than the experimental one, may be treated as a theoretical lower limit, related to a hypothetical, ideally clean crystalline material.

4. Summary

The technology of AlGaAs/InGaAs/GaAs high power, continuous-wave semiconductor laser diodes was elaborated. Heterostructures with an active region formed as a strained 8 nm thick quantum well (QW) InGaAs layer, graded composition and graded refractive index (GRIN) AlGaAs waveguide layers, were grown by molecular beam epitaxy.

Wide stripe ($W = 100$ μm) lasers revealed typical densities of the threshold current of 150 A/cm^2 and the quantum efficiencies of 0.8 W/A. In room-temperature (300 K) pulsed regime as well as continuous-wave regime, the lasers worked with guaranteed optical power of 1 W (Fig. 9). Among the two investigated types of GRINSCH structures, *i.e.*, with linear GRIN profile and with U-shaped waveguide, the first one
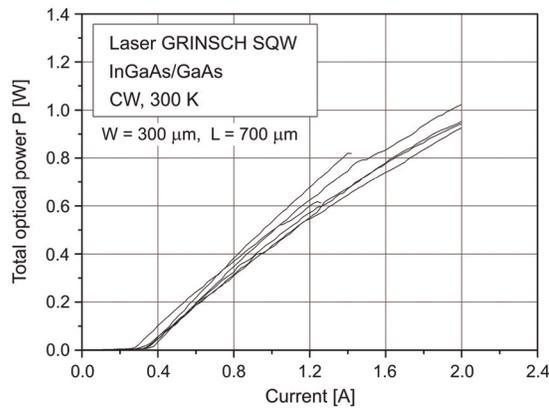
Fig. 9. Optical power-current, CW, room-temperature (300 K) characteristics, for some selected structures presented in the paper. Total power, *i.e.*, from the two mirrors, reaches 1 W for a laser chip.

exhibited lower thresholds I_{th} and higher external differential efficiencies η_{ext} and parameters T_0. This has been explained as a result of lower minority carrier concentration in the linear waveguide region.

References

[1] MROZIEWICZ B., BUGAJSKI M., NAKWASKI W., *Physics of Semiconductor Lasers*, North-Holland, 1991.

[2] CASEY H.C., PANISH M.B., JR, *Heterostructure Lasers – Principles and Applications*, Academic Press, 1978.

[3] JIN S.R., SWEENEY S.J., TOMIĆ S., ADAMS A.R., RIECHERT H., *Unusual increase of the Auger recombination current in 1.3 μm GaInNAs quantum-well lasers under high pressure*, Applied Physics Letters **82**(14), 2003, pp. 2335–7.

[4] MARKO I.P., ANDREEV A.D., ADAMS A.R., KREBS R., REITHMAIER J.P., FORCHEL A., *Importance of Auger recombination in InAs 1.3 μm quantum dot lasers*, Electronics Letters **39**(1), 2003, pp. 58–9.

[5] SWEENEY S.J., PHILIPS A.F., ADAMS A.R., O'REILLY E.P., THIJS P.J.A., *The effect of temperature dependent processes on the performance of 1.5 mm compressively strained InGaAs(P) MQW semiconductor diode lasers*, IEEE Photonics Technology Letters **10**(8), 1998, pp. 1076–8.

[6] KOSIEL K., MUSZALSKI J., SZERLING A., BUGAJSKI M., JAKIEŁA R., *Improvement of quantum efficiency of MBE grown AlGaAs/InGaAs/GaAs edge emitting lasers by optimisation of construction and technology*, Vacuum **82**(4), 2007, pp. 383–8.

[7] Li J.Z., Martinelli R.U., Khalfin V.B., Shellenbarger Z., Braun A.M., Capewell D., Willner B.I., Abeles J.H., *Growth and optimization of extremely high-pulse-power graded-index separate confinement heterostructure quantum well AlGaAs/InGaAs diode lasers with broadened waveguides*, Journal of Electronic Materials **34**(2), 2005, pp. 156–60.

[8] www.crosslight.com.